

MicroRNA-1 regulates the development of osteoarthritis in a Col2a1-Cre-ER^{T2}/GFP^{fl/fl}-RFP-miR-1 mouse model of osteoarthritis through the downregulation of Indian hedgehog expression

XIANDA CHE^{1*}, TAOYU CHEN^{1*}, LEI WEI², XIAODONG GU¹, YANGYANG GAO¹, SHUFEN LIANG¹, PENGHUA LI³, DONGPING SHI³, BIN LIANG³, CHUNFANG WANG⁴ and PENG CUI LI¹

¹Department of Orthopedics, The Second Hospital of Shanxi Medical University, Taiyuan, Shanxi 030001, P.R. China;

²Department of Orthopedics, Warren Alpert Medical School, Brown University, Providence, RI 02903, USA;

³Fengyang Hospital of Shanxi Province, Fengyang, Shanxi 032200; ⁴Laboratory Animal Center of Shanxi Medical University, Taiyuan, Shanxi 030001, P.R. China

Received October 26, 2019; Accepted April 21, 2020

DOI: 10.3892/ijmm.2020.4601

Abstract. The present study assessed the effects of microRNA-1 (miR-1) on the development of osteoarthritis using human tissues and a Col2a1-Cre-ER^{T2}/GFP^{fl/fl}-RFP-miR-1 mouse model of osteoarthritis. Human cartilage tissues (n=20) were collected for reverse transcription-quantitative polymerase chain reaction (RT-qPCR), histological analysis and immunohistochemistry experiments. A transgenic mouse model of osteoarthritis was established by subjecting Col2a1-Cre-ER^{T2}/GFP^{fl/fl}-RFP-miR-1 transgenic mice to anterior cruciate ligament transection (ACLT). Mice were subjected to radiography and *in vivo* fluorescence molecular tomography (FMT), while mouse tissues were collected for histological analysis, RT-qPCR and Safranin O staining. It was found that the miR-1 level was downregulated, whereas the levels of Indian hedgehog (Ihh), as well as those of its downstream genes were upregulated in human osteoarthritic cartilage. In the transgenic mice, treatment with tamoxifen induced miR-1, as well as collagen, type II (Col2a1) and Aggrecan (Acan) expression; however, it decreased Ihh, glioma-associated oncogene homolog (Gli)1, Gli2, Gli3, smoothened homolog (Smo), matrix metalloproteinase (MMP)-13 and collagen type X (Col10) expression. Safranin O staining revealed cartilage surface damage in the non-tamoxifen + ACLT group, compared with that in the tamoxifen + ACLT group. Histologically, an

intact cartilage surface and less fibrosis were observed in the tamoxifen + ACLT group. Immunohistochemistry revealed that the protein expression of Ihh, Col10, and MMP-13 was significantly higher in the joint tissues of the non-tamoxifen + ACLT group than in those of the tamoxifen + ACLT group. However, Col2a1 expression was lower in the joint tissues of the non-tamoxifen + ACLT group than in those of the tamoxifen + ACLT group. The results of RT-qPCR and FMT further confirmed these findings. On the whole, the findings of the present study demonstrate that miR-1 expression protects against osteoarthritis-induced cartilage damage and gene expression by inhibiting Ihh signaling.

Introduction

Osteoarthritis is a common joint disease affecting elderly individuals that induces joint pain and stiffness, thus severely affecting the quality of life of these individuals (1). The incidence rate of osteoarthritis among Asians aged ≥65 years is predicted to more than double from 6.8% in 2008 to 16.2% in 2040. In addition, due to an increase in the incidence of sports-associated trauma, the average age of patients with osteoarthritis is estimated to decrease (2). As a chronic joint disease, osteoarthritis is often characterized by articular cartilage degeneration and osteophyte formation. The lack of an articular cartilage blood supply, neural control and lymphatic vessels render the repair of this type of damage difficult (3). To date, the precise pathogenesis and molecular mechanisms responsible for the development and progression of osteoarthritis remain unclear; thus, there is no effective method yet available for the prevention or treatment of osteoarthritis. The risk factors of osteoarthritis include previous joint injury, abnormal joint or limb development and genetic background, as well as being overweight or having a job which requires the lifting of heavy objects, in which the mechanical stress on the joints and low-grade inflammation cause degenerative joint disease, such as osteoarthritis (4). Therefore, further studies

Correspondence to: Dr Pengcui Li, Department of Orthopedics, The Second Hospital of Shanxi Medical University, 382 Wuyi Road, Taiyuan, Shanxi 030001, P.R. China
E-mail: lpc1977@163.com

*Co-first authorship

Key words: osteoarthritis, miR-1, Indian hedgehog, transgenic mice

on the molecular pathogenesis of osteoarthritis may aid in the development of novel approaches with which to prevent and control this disease in order to improve the quality of life of affected individuals.

Recently, microRNAs (miRNAs or miRs) in the cartilage under conditions of homeostasis and osteoarthritis have gained increasing attention. miRNAs are a class of endogenous non-coding RNAs of 18-24 nucleotides in length that post-transcriptionally regulate the expression of protein-coding genes. miRNAs can recognize and bind to the 3'-untranslated region of gene transcripts (mRNA) through base complementary pairing to guide the RNA-induced silencing complex and degrade the target mRNA or repress translation of the target mRNA (5-7). Previous studies have demonstrated that both miR-140 and miR-146a are involved in the pathogenesis of osteoarthritis, thus suggesting that miRNAs play an important role in cartilage homeostasis (8-12). A more recent study revealed that miR-1 inhibited the ossification of the posterior longitudinal ligament via the MALAT1/miR-1/Cx43 regulatory axis in patient ligament samples (13). However, the role of miR-1 in the development of osteoarthritis remains unknown. A recent study demonstrated that miR-1 was highly expressed in the hypertrophic zone of growth plate cartilage, and regulated chondrocyte phenotypes during growth plate development (14). Therefore, it was hypothesized that miR-1 regulates chondrocyte homeostasis. Previous studies have revealed that both miR-1 and Indian hedgehog (Ihh) are distributed in the pre-hypertrophic region of cartilage tissues (11,14,15). This region is involved in chondrocyte hypertrophy, suggesting that miR-1 and Ihh play a role in chondrocyte homeostasis.

Indeed, Ihh is involved in cartilage degeneration and osteoarthritis progression (16). It has been demonstrated that chondrocytes undergo hypertrophic differentiation in the early stages of osteoarthritis (17,18), while Ihh functions to regulate chondrocyte hypertrophy, thereby achieving endochondral ossification (19-21). It was previously demonstrated that the disruption of the Ihh signaling pathway *in vivo* was able to attenuate osteoarthritis progression in a transgenic mouse *Ihh^{fl/fl}* model of osteoarthritis induced by surgery (22), while Ipriflavone was able to reduce cartilage degeneration in rats by blocking Ihh signaling (23). Thus, the upregulation of the Ihh pathway plays an important role in osteoarthritis progression, whereas the inhibition of the Ihh pathway attenuates cartilage degradation.

In the present study, the levels of miR-1 and Ihh were first assessed in the tibial plateau of humans with or without osteoarthritis, and a transgenic mouse model of osteoarthritis was then established after subjecting Col2a1-Cre-ER^{T2}/GFP^{fl/fl}-RFP-miR-1 transgenic mice to anterior cruciate ligament transection (ACLT) (24,25). The effects of miR-1 expression in mice on the regulation of Ihh, glioma-associated oncogene homolog (Gli)1, Gli2, Gli3, smoothened homolog (Smo), MMP-13, collagen type X (Col10), Col2a1 and Aggrecan (Acan) expression were also analyzed.

Materials and methods

Human cartilage tissues. The present study was approved (2019YX260) by the Institutional Ethics Committee of the

Second Hospital of Shanxi Medical University (Taiyuan, China), and all patients provided informed consent. Cartilage tissues (n=20) were obtained from the cartilage samples of the tibial plateau during total knee arthroplasty of patients with osteoarthritis who were diagnosed according to the American Rheumatism Association Criteria for osteoarthritis (26). Histologically, these cartilage samples exhibited severe damage and were harvested from the medial region of the tibial plateau, while the relatively normal cartilage was harvested from the normal appearing non-loaded area of the tibial plateau of the same patient as a control (normal). These cartilage tissue samples after harvest were ground in liquid nitrogen using a mortar and pestle and used for reverse transcription-quantitative PCR (RT-qPCR), while the articular cartilage tissue sections were processed and stained by Safranin O/fast green or immunohistochemistry.

RT-qPCR. The whole-knee cartilage was first dissected with a scalpel and then ground in liquid nitrogen, and total cellular RNA was isolated from the human and mouse samples (for mouse samples, please see below) using TRIzolTM reagent (Invitrogen; Thermo Fisher Scientific, Inc.), according to the manufacturer's instructions. The cartilage samples from 3 mice were pooled together, and 3 pooled samples per group were used for RNA isolation. These RNA samples were then subjected to reverse transcription into complementary DNA (cDNA) using PrimeScriptTM RT Master Mix (Takara Bio, Inc.). Total cellular miRNA was isolated from these human and mouse cartilage samples using the miRNeasy Mini kit (Qiagen), according to the manufacturer's protocol, and reverse transcribed into cDNA using the MiScript Reverse Transcription kit (Qiagen). rRNA 18s and U6 were used as internal controls for mRNA and miRNA, respectively. The stem-loop primers for miR-1 were purchased from Qiagen. These cDNA samples were then subjected to qPCR amplification using the TB GreenTM Premix Ex TaqTM II kit (Takara) with the Applied BiosystemsTM QuantStudioTM 6 Flex real-time PCR system (Applied Biosystems; Thermo Fisher Scientific, Inc.). The qPCR conditions were as follows: Pre-incubation of samples at 50°C for 2 min and 95°C for 10 min, and then 40 cycles of denaturation at 95°C for 10 sec, annealing at 55°C for 30 sec, and extension at 72°C for 30 sec. The level of each transcript was quantified by using the threshold cycle (Ct) 2^{-ΔΔCt} method (27). The primer sequences are presented in Table I.

Animals and care. The animal protocol of the present study was approved (SYDL2019010) by the Institutional Animal Care and Use Committee (IACUC) of The Second Hospital of Shanxi Medical University (Taiyuan, China) and following the Guidelines of the Care and Use of Laboratory Animals issued by the Chinese Council on Animal Research. A total of 92 mice of 2-months age were maintained in a specific pathogen-free (SPF) 'barrier' facility and housed under controlled temperature and humidity and alternating 12-h light and dark cycles. The mice received SPF mouse chow and were provided with sterile drinking water *ad libitum*. During the experiment, the behavior and health of the mice were monitored daily and recorded every 3 days. The mice were anesthetized with pentobarbital sodium by an intra-

Table I. Primers for used for RT-qPCR.

Species	Gene	DNA sequence
Mouse	Col2a1	5'-AAGGGACACCGAGGTTTCACTGG-3' 5'-GGGCCTGTTTCTCCTGAGCGT-3'
	Col10	5'-GCCAGGAAAGCTGCCCCACG-3' 5'-GAGGTCCGGTTGGGCCTGGT-3'
	Acan	5'-CAGTGGGATGCAGGCTGGCT-3' 5'-CCTCCGGCACTCGTTGGCTG-3'
	MMP-13	5'-GGACCTTCTGGTCTTCTGGC-3' 5'-GGATGCTTAGGGTTGGGGTC-3'
	Ihh	5'-CCACTTCCGGGCCACATTTG-3' 5'-GGCCACCACATCCTCCACCA-3'
	Gli1	5'-GGTCCGGATGCCACGTGAC-3' 5'-TCCCGCTTGGGCTCCACTGT-3'
	Gli2	5'-TGGCAGCGATGGGCCTACCT-3' 5'-GTGTGCTGCTGTTTGGC-3'
	Gli3	5'-CATGAACAGCCCTTTAAGAC-3' 5'-TCATATGTGAGGTAGCACCA-3'
	Smo	5'-CTCCTACTTCCACCTGCTCAC-3' 5'-CAAAACAAATCCCACTCACAGA-3'
	COL2A1	5'-TGAGGGCGCGGTAGAGACCC-3' 5'-TGCACACAGCTGCCAGCCTC-3'
	COL10	5'-TGCCCTTGTGTCAGTGCTAACC-3' 5'-GCGTGCCGTTCTTATACAGG-3'
	Acan	5'-CATTCAACAGTGAGGACCTCGT-3' 5'-TCACACTGCTCATAGCCTGCTTC-3'
	MMP-13	5'-TGCTGCATTCTCCTTCAGGA-3' 5'-ATGCATCCAGGGGTCTTGGC-3'
	Ihh	5'-ATCATCTTCAAGGACGAGGAGA-3' 5'-GGGCCTTTGACTCGTAATACAC-3'
Human	Gli1	5'-GAACCCTTGGAAGGTGATATGTC-3' 5'-GGCAGTCAGTTTCATACACAGAT-3'
	Gli2	5'-GCGTGTTTACCCAATCCTGT-3' 5'-GATGCTCCCTCAGAGTCCTG-3'
	Gli3	5'-CTTTGCAAGCCAGGAGAAAC-3' 5'-TTGTTGGACTGTGTGCCATT-3'
	Smo	5'-CCTTTGGCTTTGTGCTCATTACCTT-3' 5'-CGTCACTCTGCCCAGTCAACCT-3'
	18s	5'-CGGCTACCACATCCAAGGAA-3' 5'-GCTGGAATTACCGCGGCT-3'

RT-qPCR, reverse transcription-quantitative polymerase chain reaction; COL(Col), collagen; Acan, Aggrecan; MMP-13, matrix metalloproteinase-13; Ihh, Indian hedgehog; Gli, Glioma-associated oncogene homolog; Smo, smoothened homolog.

peritoneal injection (35 mg/kg). Mice were then euthanatized using 100% CO₂ when the following humane endpoints were reached: i) The mice experienced weight loss (15-20% of their original body weight rapidly decreased); ii) anorexia (no food at all for 24-36 h); iii) weakness (unable to eat and drink on their own); and iv) infection of body organs (penicillin treatment not effective). Following euthanasia, the death of the mice was confirmed by continuous non-breathing for 2-3 min, no heartbeat and no blink reflex.

Transgenic mice and surgical induction of osteoarthritis with ACLT. Col2a1-Cre-ER^{T2}/GFP^{fl/fl}-RFP-miR-1 transgenic mice with conditional miR-1 overexpression were generated at the Department of Orthopedics, Warren Alpert Medical School, Brown University and were provided by the Department of Orthopedics, Warren Alpert Medical School, Brown University. Specifically, Col2a1-Cre-ER^{T2} mice were mated with GFP^{fl/fl}-RFP-miR-1 mice to obtain next-generation mice with the Col2a1-Cre-ER^{T2}/GFP^{fl/fl}-RFP-miR-1 genotype.

To stimulate tamoxifen-induced CreERT2 recombinase and miR-1 expression in the cartilage, the mice were intraperitoneally injected with tamoxifen (100 $\mu\text{g/g}$ body weight/day for 5 consecutive days), as described in a previous study (11).

In the present study, 5 of wild-type C57BL/C mice and 5 transgenic mice were utilized, at 2 months old. These mice were photographed, X-ray detected, and the knee joints were then harvested following euthanasia for Safranin O staining to assess the phenotypic differences between the transgenic and wild-type mice. Furthermore, 20 of transgenic mice were utilized, at 2 months old, and were randomly divided into the tamoxifen (intraperitoneal injection) or control group (intraperitoneal injection of corn oil; $n=10/\text{group}$). The mice were euthanized at 3 months of age, and the knee joints were then harvested for RT-qPCR to assess the levels of miR-1 and Ihh. In addition, another 60 of these transgenic mice were selected, aged 2 months old, and were randomly divided into the following 4 groups ($n=15/\text{group}$): Non-tamoxifen + ACLT, non-tamoxifen + Sham (sham-operated), tamoxifen + ACLT, tamoxifen + Sham. Tamoxifen was intraperitoneally injected into 2-month-old mice (100 $\mu\text{g/g}$ body weight/day for 5 consecutive days), while ACLT was conducted in 3-month-old mice. The surgery was conducted on the right knees of the mice; 2 months later, these mice were euthanized and the right hind limbs were harvested immediately for further analyses.

Radiography. Small-animal X-ray radiography was performed to detect the changes in the knee joints of these mice at 2 months after surgery using a small-animal X-ray apparatus (UltraFocus, Faxitron). In brief, the X-ray films were acquired at the anteroposterior and lateral positions of the mice under anesthesia (pentobarbital sodium by an intraperitoneal injection; 35 mg/kg), and the exposure time and kV were set to the auto setting.

Histological evaluation. At 2 months after the different procedures, the knee joint of the right hind limb was harvested and fixed in 4% buffered paraformaldehyde for 48 h and decalcified in a 10% ethylenediaminetetraacetic acid solution (pH 7.2) for 8 weeks. These samples underwent routine tissue processing and were then embedded in paraffin and sectioned in the coronal orientation using a rotary microtome (Leica Microsystems GmbH) to provide 6- μm -thick coronal sections. Following deparaffinization in xylene and rehydration in graded ethanol solutions and then in H_2O , the sections were stained with Safranin O/Fast Green (Sigma-Aldrich; Merck KGaA). The sections were reviewed and scored for cartilage degradation by 2 pathologists who were without knowledge of the study groups, according to The International Association of Osteoarthritis Research (OARSI) grading system (28). The score ranged from 0 to 6, with a higher score indicating more severe degradation.

Immunohistochemistry. Paraffin-embedded sections of these mouse tissue specimens were immunostained for the expression of Ihh, MMP-13, Col10 and Col2a1. The deparaffinized and rehydrated sections were incubated in 3% H_2O_2 in phosphate-buffered saline (PBS) to block any endogenous peroxidase activity at room temperature for 10 min. The sections were washed with PBS and digested with 0.1% trypsin

at 37°C for 30 min to expose antigens that may be blocked by tissue fixation and processing. Subsequently, the sections were incubated with 20% normal serum at room temperature for 30 min and then with anti-mouse Col2a1 (1:100; cat. no. ab34712; Abcam), anti-Col10 (1:100; cat. no. BA2023; Wuhan Boster Biological Technology, Ltd.), anti-Ihh (1:50; cat. no. bs-6624R; BIOSS), or anti-MMP-13 (1:100; cat. no. ab39012; Abcam) at 4°C overnight. The sections were then washed 3 times with PBS and were then incubated with a horseradish peroxidase-conjugated secondary antibody (Stock solution; cat. no. PV-9001; ZSGB-BIO) at 37°C for 30 min; the color reaction was conducted by brief incubation of the sections in 3,3'-diaminobenzidine solution. The immunostained sections were reviewed and photographed under a Leica DM6B microscope (Leica Microsystems GmbH) for quantitation.

Fluorescence molecular tomography (FMT). FMT is a sensitive and quantitative technique that provides 3-dimensional tissue images *in vivo* (29,30). The FMT 4000 *In Vivo* Imaging System from PerkinElmer, Inc. was utilized to monitor the levels of MMPs and cathepsins in the mouse knee joints at 2 months after surgery. The mice received a single dose of MMPsense 645 FAST Fluorescent Imaging Agent (10 μl , 0.4 nmol; PerkinElmer, Inc.) and ProSense 750 FAST (10 μl , 0.4 nmol; PerkinElmer) via tail vein injection at 24 h before imaging. MMPsense is able to detect MMP-2, MMP-3, MMP-7, MMP-9, MMP-12 and MMP-13, while ProSense can detect cathepsins B, L, S, K, V and D, as well as plasmin. The concentrations of MMPs and PRO probes in the mouse knee joints were calculated by using the region of the interest method, and the data are expressed as the means \pm standard deviation (SD; $n=5$ mice per group).

Statistical analysis. The data are expressed at the means \pm SD and statistically analyzed by using SPSS software (version 19.0; IBM Corporation) and Graph Prism Software (version 5.0; Graph Prism Software, Inc.). The comparisons of 2 groups of samples were analyzed by two-way analysis of variance followed by Tukey's test. A Kruskal-Wallis analysis with post-hoc Dunn's test was performed to test differences in OARSI grading score between groups. A P-value ≤ 0.05 was considered to indicate a statistically significant difference.

Results

Downregulation of miR-1 and upregulation of Ihh levels in human osteoarthritic cartilage. In the present study, the miR-1 and Ihh levels were first assessed in osteoarthritic cartilage by RT-qPCR. The data revealed that the normal samples expressed higher levels of miR-1 (hsa-miR-1-5p; $P=0.009$), COL2A1 ($P=0.016$), and Acan ($P=0.025$), whereas they exhibited lower levels of Ihh ($P=0.017$), Gli2 ($P=0.027$), Gli3 ($P=0.024$), Smo ($P=0.001$), MMP-13 ($P=0.005$) and COL10 ($P=0.014$), compared with those of the osteoarthritis group (Fig. 1A and B). However no marked differences were observed in the Gli1 level ($P=0.058$) between the normal and diseased samples. The results of immunohistochemistry revealed that the expression of Ihh and MMP-13 was markedly higher in the osteoarthritis group than in the normal group (Fig. 1C).

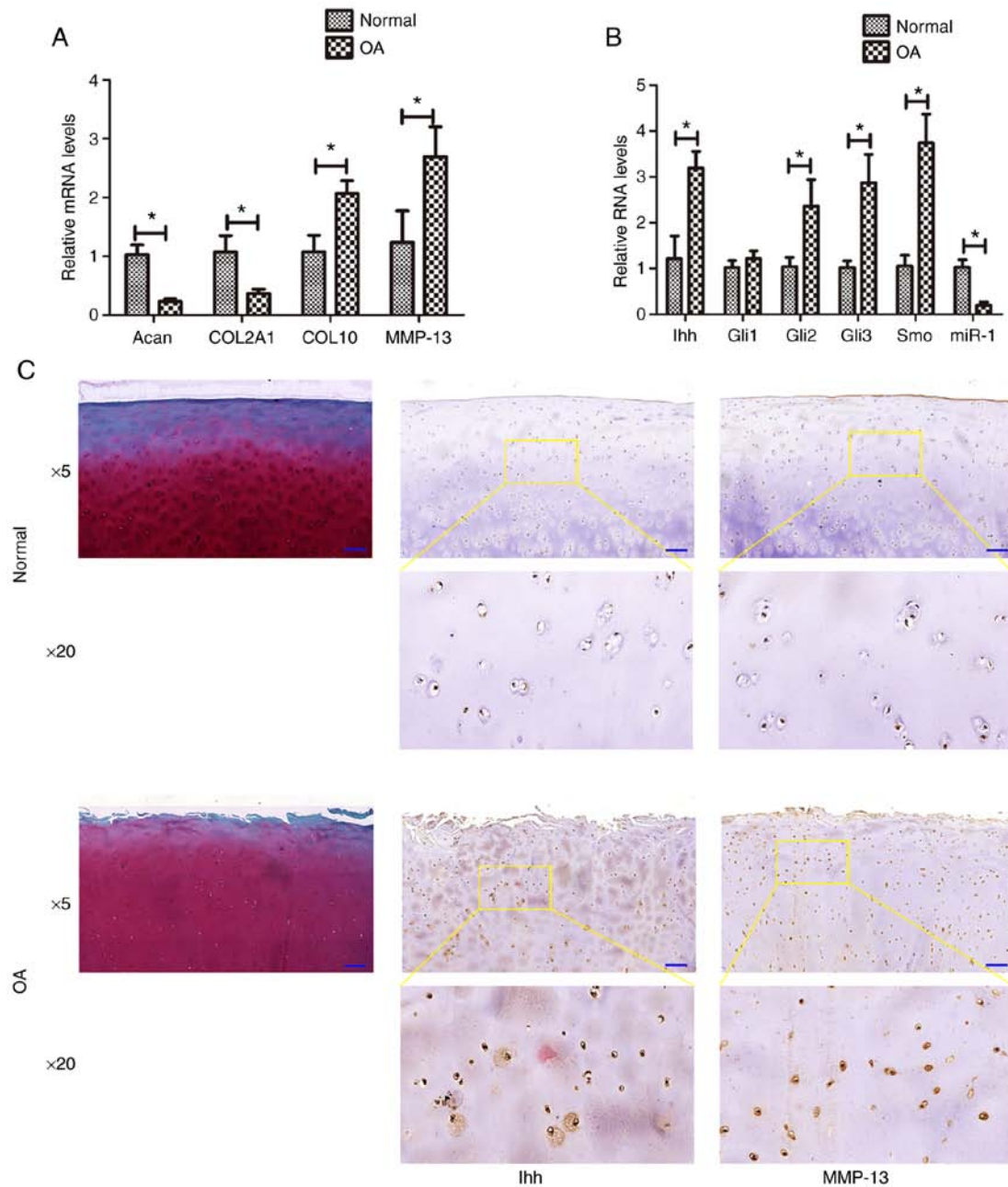


Figure 1. Downregulation of miR-1 and upregulation of Ihh levels in human osteoarthritic cartilage. (A and B) RT-qPCR. Human osteoarthritic cartilage and adjacent normal cartilage were collected and subjected to RT-qPCR analysis of miR-1. * $P < 0.05$. (C) Safranin O staining and immunohistochemistry. Human osteoarthritic cartilage and adjacent normal cartilage were collected and subjected to the staining procedure (blue scale bar: 200 μ m). OA, osteoarthritis; Acan, Aggrecan; COL2A1, collagen, type II; COL10, collagen type X; MMP, matrix metalloproteinase; Ihh, Indian hedgehog; Gli, glioma-associated oncogene homolog; Smo, smoothened homolog.

Characteristics of transgenic mice. Subsequently, Col2a1-Cre-ER^{T2}/GFP^{fl/fl}-RFP-miR-1 mice were successfully generated (Fig. 2A) and the presence of miR-1 and Col2a1-Cre was confirmed by genotyping (Fig. 2B). In particular, prior to the tamoxifen injection, the transgenic and wild-type mice at 2 months of age exhibited no differences in phenotype, with the mice exhibiting a similar body type, X-ray appearance and normal Safranin O staining (Fig. 2C). However, following the tamoxifen injection, the transgenic mice exhibited lower levels of Ihh ($P = 0.024$), Gli2 ($P = 0.004$), Gli3 ($P = 0.006$), Smo ($P = 0.002$), MMP-13 ($P = 0.016$) and Col10 ($P = 0.027$); however, they exhibited elevated levels of Col2a1 ($P = 0.006$) and Acan

($P = 0.036$) expression, compared with those in the non-tamoxifen-injected mice; of note, the level of Gli1 ($P = 0.009$) did not differ significantly between the groups. Moreover, the level of miR-1 (mmu-miR-1a-5p; $P = 0.004$) expression was evaluated, indicating the successful generation of these transgenic mice (Fig. 2D and E).

Transgenic mouse model of osteoarthritis. A transgenic mouse model of osteoarthritis was then established by subjecting mice to ACLT. At 2 months after ACLT, X-ray examination of the knee joints revealed that the patella, tibial plateau and tibial intercondylar formed osteophytes in the non-tamoxifen + ACLT

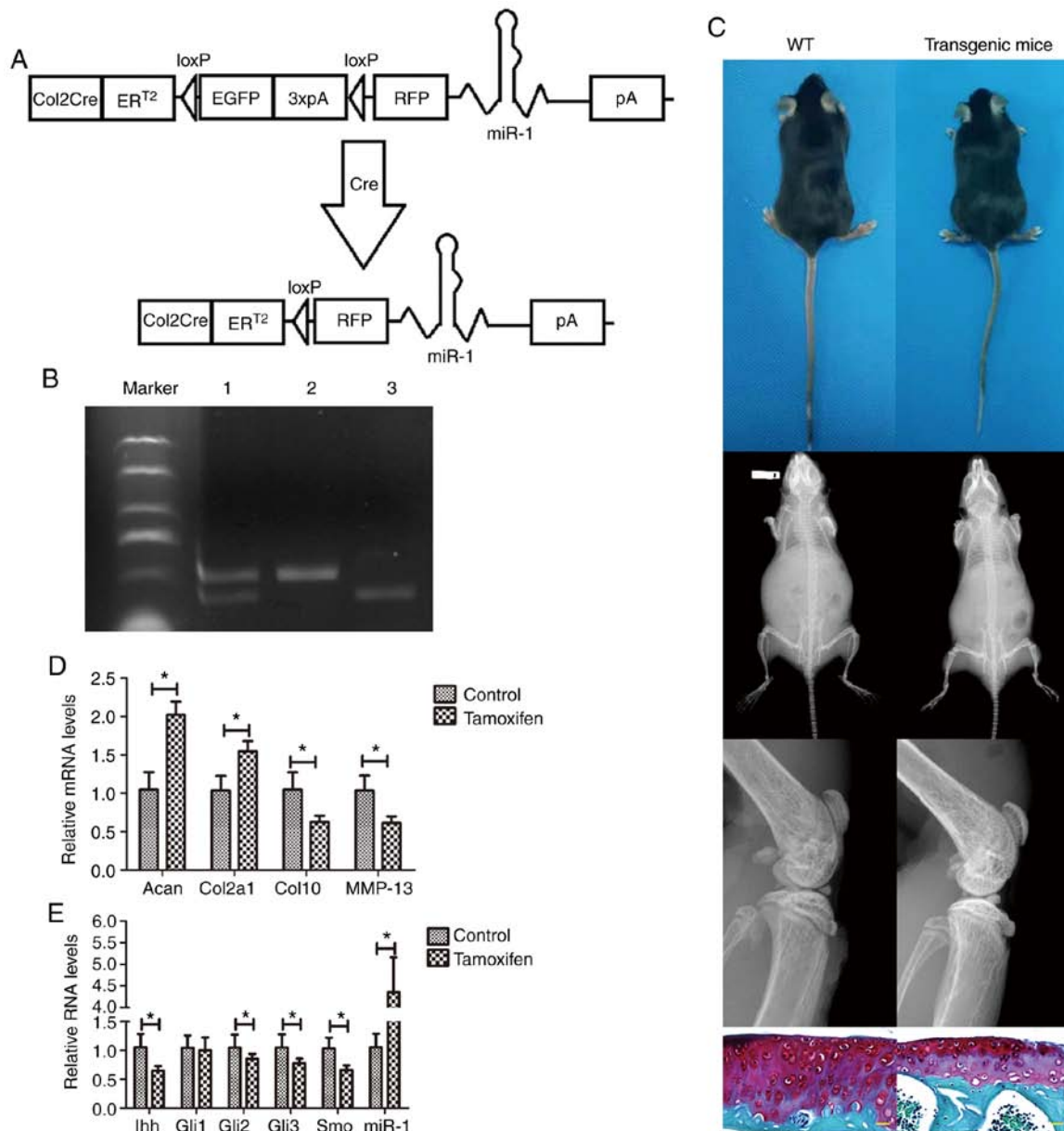


Figure 2. Transgenic mouse model of osteoarthritis. (A) Illustration of the Col2a1-Cre-ER^{T2}/GFP^{fl/fl}-RFP-miR-1 mice. (B) DNA gel electrophoresis showing the insertion of the loxP restriction enzyme site in the miR-1 allele confirmed by PCR. Lane 1, miR-1 and Col2a1-Cre (300 bp and 450 bp); lane 2, Col2a1-Cre (450 bp); lane 3, miR-1 (300 bp). (C) X-ray radiography and Safranin O staining (yellow scale bar: 20 μ m). (D and E) RT-qPCR. Mouse cartilage samples from tamoxifen-treated mice and control mice were collected 8 weeks after the surgery and subjected to RT-qPCR analysis. * $P < 0.05$. WT, wild-type; Acan, Aggrecan; Col2a1, collagen, type II; Col10, collagen type X; MMP, matrix metalloproteinase; Ihh, Indian hedgehog; Gli, glioma-associated oncogene homolog; Smo, smoothened homolog.

group, and the joint space was narrowed; by contrast, in the tamoxifen + ACLT group, although there were osteophytes, there were no evident changes in these joints, and the joint space was also normal (Fig. 3). In addition, there was no obvious osteophyte formation in the 2 sham-operated groups.

Subsequently, the articular cartilage was stained with Safranin O for the visualization of glycosaminoglycans. Cartilage surface damage, as well as weaker Safranin O staining was observed in the non-tamoxifen + ACLT group, compared with that in the tamoxifen + ACLT group (Fig. 4A). Histologically, there was an intact cartilage surface and less fibrosis in the tamoxifen + ACLT group. The OARS grading score was significantly higher in the non-tamoxifen + ACLT group (2.52 ± 0.24), compared with the tamoxifen + ACLT

group (0.57 ± 0.14 ; $P < 0.05$; Fig. 4B), indicating more severe degradation and damage in the non-tamoxifen + ACLT group.

miR-1 inhibits Ihh expression and cartilage catabolism, whereas it promotes anabolism in the transgenic mouse model of osteoarthritis. Immunohistochemistry revealed that the protein expression of Ihh, Col10 and MMP-13 was markedly higher in the joint tissues of the non-tamoxifen + ACLT group than in those of the tamoxifen + ACLT group (Fig. 5). However, Col2a1 expression was lower in the joint tissues of the non-tamoxifen + ACLT group than in those of the tamoxifen + ACLT group (Fig. S1).

Furthermore, the RT-qPCR data confirmed the immunohistochemical data (Fig. 4C and D), indicating that the joint



Figure 3. X-ray radiography analysis of the mouse knee joints at eight weeks after ACLT. The data show significant changes in osteophyte formation along the patella, tibial plateau, and tibial intercondylar eminence in the transgenic mouse model of osteoarthritis compared with that of the miR-1-overexpressed ACLT mice (black arrow heads). In contrast, there was no obvious osteophyte formation in the two sham-operated mice. Sham, sham-operated; ACLT, anterior cruciate ligament transection.

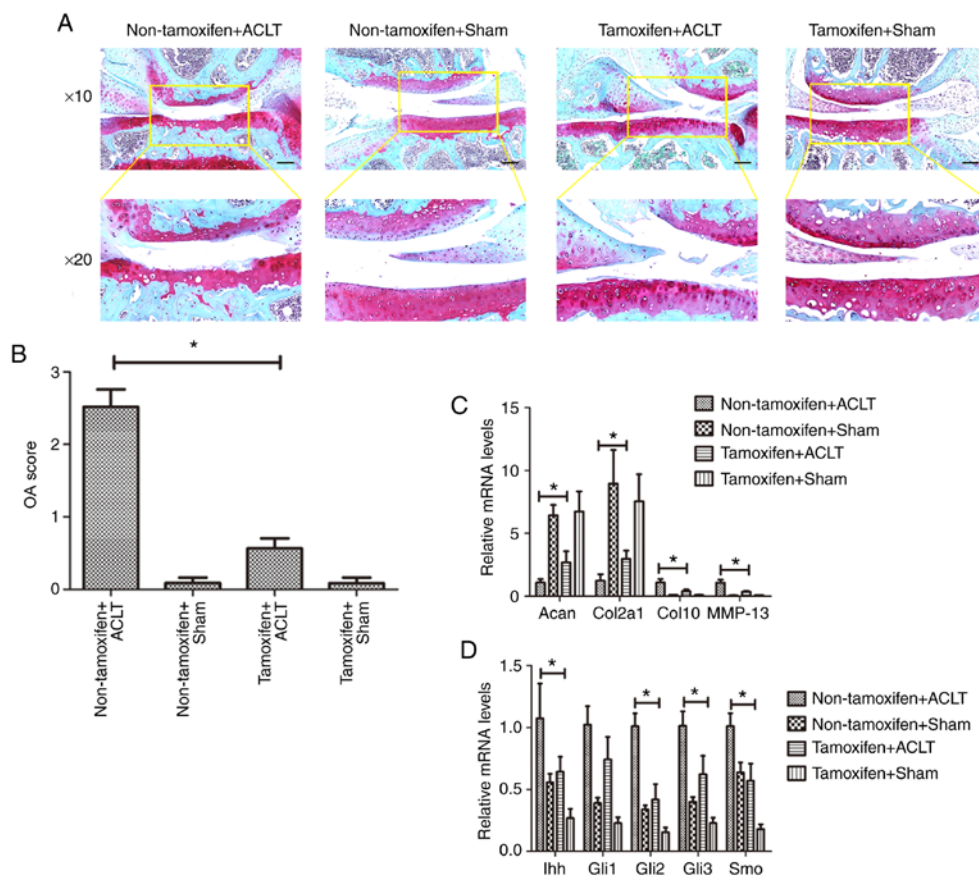


Figure 4. Effect of miR-1 overexpression on the inhibition of disease progression in the transgenic mouse model of osteoarthritis. (A) Safranin O staining. Mouse tissues were collected at 8 weeks after ACLT and subjected to Safranin O staining (black scale bar: 100 μ m). The images the bottom panels are magnified images of the are in the yellow boxes in the top panels. (B) OARSI scores. (C and D) RT-qPCR. Mouse tissues were collected at 8 weeks after ACLT and subjected to RT-qPCR analysis. * $P < 0.05$. Sham, sham-operated; ACLT, anterior cruciate ligament transection; Acan, Aggrecan; Col2a1, collagen, type II; Col10, collagen type X; MMP, matrix metalloproteinase; Ihh, Indian hedgehog; Gli, glioma-associated oncogene homolog; Smo, smoothened homolog.

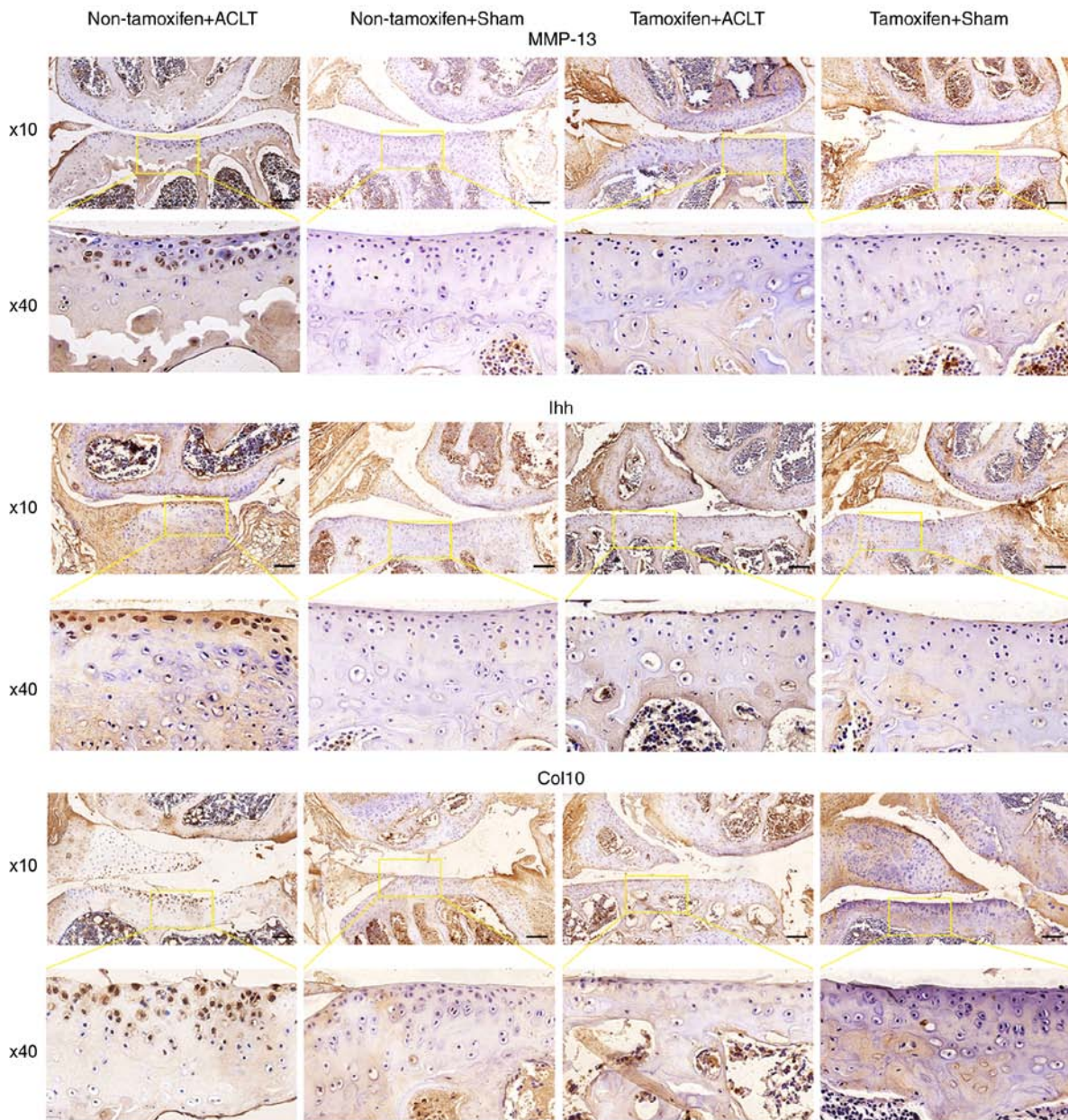


Figure 5. Expression of different proteins in the transgenic mouse model of osteoarthritis. Mouse tissues were collected at 2 months after ACLT and then subjected to tissue processing and immunohistochemistry (black scale bar: 100 μ m). The images the bottom panels are magnified images of the are in the yellow boxes in the top panels. Sham, sham-operated; ACLT, anterior cruciate ligament transection; MMP, matrix metalloproteinase; Col10, collagen type X; Ihh, Indian hedgehog.

tissues of the tamoxifen + ACLT group expressed lower levels of Ihh ($P=0.026$), Gli2 ($P=0.028$), Gli3 ($P=0.004$), Smo ($P=0.001$), MMP-13 ($P=0.010$) and Col10 ($P=0.004$); however, they expressed higher levels of Col2a1 ($P=0.012$) and Acan ($P=0.035$), compared with those of the non-tamoxifen + ACLT group; the Gli1 ($P=0.061$) level did not differ significantly between the 2 groups.

In addition, FMT with the appropriate probes was used to monitor the levels of MMPs and cathepsins in the knees of alive mice (Fig. 6). The data revealed that the MMP level was significantly lower in the tamoxifen + ACLT group (3.74 ± 0.45 pmol) than in the non-tamoxifen + ACLT group (8.20 ± 1.51 pmol; $P<0.001$). Moreover, the cathepsin level was also significantly lower (6.36 ± 1.80 pmol) in the tamoxifen + ACLT group than in the non-tamoxifen + ACLT group (16.18 ± 4.42 pmol; $P=0.016$),

further confirming the immunohistochemistry and RT-qPCR results.

Discussion

miRNAs post-transcriptionally regulate gene expression and control a wide range of biological processes in cells and tissues (31). miR-1 plays a role in myocyte proliferation and differentiation (32), as well as in the growth of growth plate chondrocytes during development (14). In the present study, it was found that miR-1 expression was low in human osteoarthritic joint tissues and that miR-1 induction was able to suppress osteoarthritis in a Col2a1-Cre-ER^{T2}/GFP^{fl/fl}-RFP-miR-1 mouse model of osteoarthritis. Furthermore, Ihh is a secreted protein that is expressed in pre-hypertrophic chondrocytes (33),

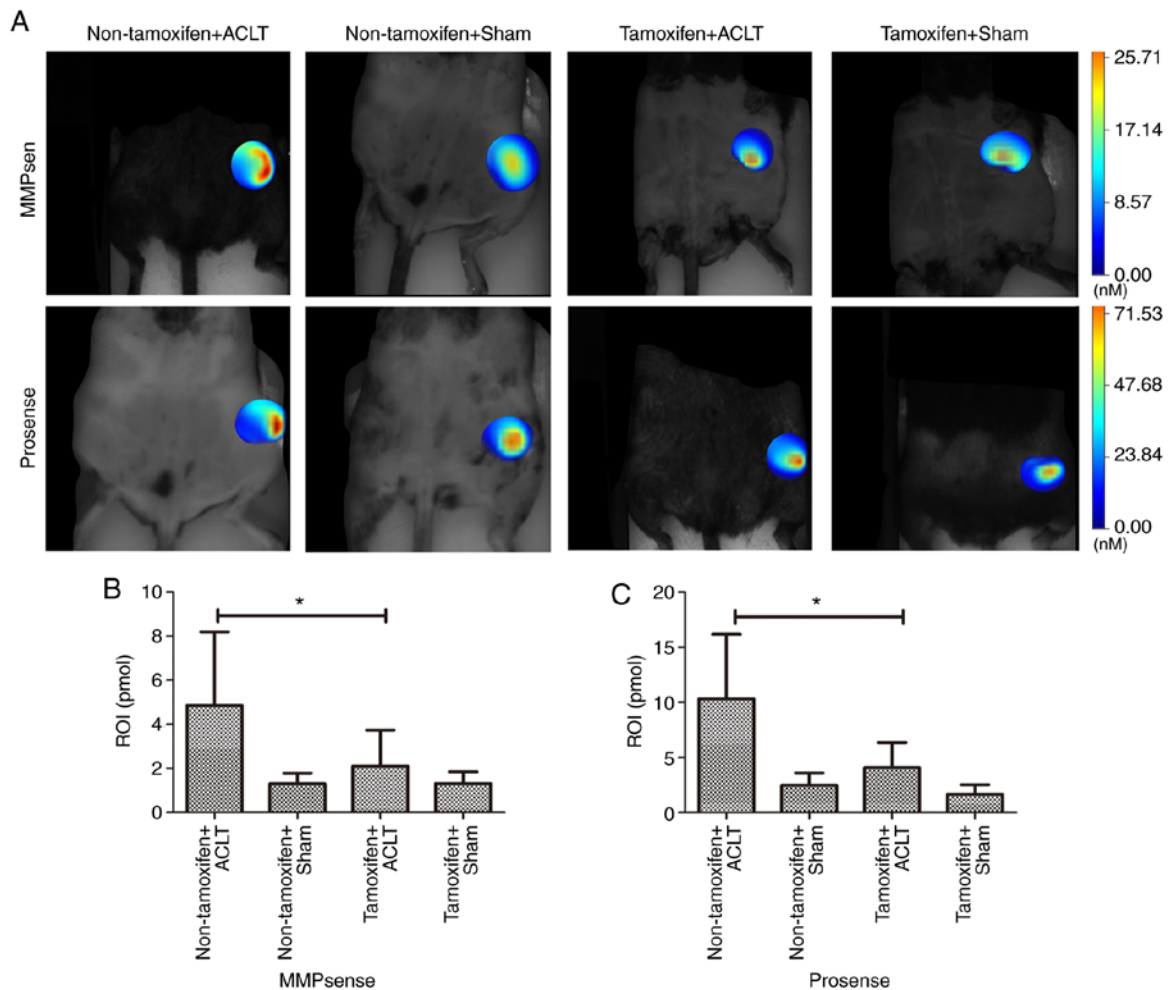


Figure 6. The *in vivo* FMT measurement of total MMPs and cathepsins in the transgenic mouse model of osteoarthritis. These mice were subjected to *in vivo* FMT at 2 months after ACLT. (A and B) Detection of the MMP level in the mice. The graph summarizes the FMT data. (A and C) Detection of the cathepsin level in the mice. The graph summarizes the FMT data (n=5 per group). *P<0.05. Sham, sham-operated; ACLT, anterior cruciate ligament transection; MMP, matrix metalloproteinase.

indicating that the upregulation of *Ihh* can promote the hypertrophic phenotype and induce the expression of typical hypertrophic markers, such as COL10 and MMP-13 (10). Thus, upregulated *Ihh* signaling can contribute to the development of osteoarthritis (34-37). In the present study, it was revealed that the miR-1-induced inhibition of *Ihh* (data not shown) signaling was able to suppress the development of osteoarthritis in a Col2a1-Cre-ER^{T2}/GFP^{fl/fl}-RFP-miR-1 mouse model of osteoarthritis. Specifically, it was found that *Ihh* expression was low in normal human articular cartilage, whereas it was increased in osteoarthritis-damaged cartilage. *Ihh* expression was associated with the severity of osteoarthritis, in terms of cartilage damage, thus confirming previous observations and analyses of human samples (10,38). The expression of miR-1 was inversely proportional to that of *Ihh* in human osteoarthritis-damaged articular cartilage. Therefore, the development of therapies that target *Ihh* may be a novel approach for the treatment or prevention of osteoarthritis.

Indeed, the transgenic mouse model of osteoarthritis is a useful tool with which to assess the effects of miR-1 on the regulation of osteoarthritis development and treatment. In the current study, Col2a1-Cre-ER^{T2}/GFP^{fl/fl}-RFP-miR-1 mice were obtained and generated a transgenic mouse model of osteo-

arthritis was then established following surgical ACLT. Mouse cartilage was then resected for the assessment of osteoarthritis by radiography, histology, gene expression and Safranin O staining. The X-ray examination of the knee joints of mice at 2 months following ACLT revealed that the patella, tibial plateau and tibial intercondylar formed osteophytes in osteoarthritic mice and that the joint space was narrowed; whereas ACLT mice with miR-1 overexpression had no obvious changes in these joints or the joint space. Safranin O staining of the articular cartilage revealed more cartilage surface damage in the osteoarthritic mice compared with that in the ACLT mice with miR-1 overexpression. Histologically, the mice subjected to ACLT with miR-1 overexpression had an intact cartilage surface with less fibrosis. These data clearly revealed the role of miR-1 in the control of osteoarthritis development in these mice.

The data of the present study also demonstrated that the levels of *Ihh* and its downstream genes (such as *Gli2*, *Gli3*, and *Smo*), MMP-13 and Col10 were lower in the miR-1-overexpressing cartilage, whereas the levels of Col2a1 and *Acan* were higher. These findings were further confirmed by the immunohistochemistry and FMT data. FMT is an advanced, sensitive bioimaging method that provides noninvasive, in-depth tissue imaging and quantification of *in vivo*

biological targets (10). In the present study, *in vivo* FMT was performed and it was found that the expression of MMPs and cathepsins was downregulated in miR-1-overexpressing mice subjected to ACLT compared to that of osteoarthritic mice. These findings were consistent with the immunohistochemistry and RT-qPCR results.

However, the present study does have some limitations; for example, the reason why there was no change in Gli1 expression between the normal and osteoarthritic human samples or between the tissues from osteoarthritic and miR-1-overexpressed ACLT mice cannot be explained. Moreover, the direct miR-1 binding or regulation of Ihh expression was not confirmed, although in another study by the authors, bioinformatics analysis of miR-1 target genes using TargetScan (<http://www.targetscan.org>) and miRanda (<http://www.microrna.org>) revealed that there are two specific binding sites (miRBase Accession no. #MIMAT0000416) between miR-1 and the 3'-untranslated region of Ihh (unpublished data). Further research using a luciferase reporter assay is required to validate their direct interaction.

In conclusion, the present study revealed that miR-1 plays an important role in protection of the articular cartilage from osteoarthritis-induced degeneration and is accompanied by the downregulation of Ihh expression. Future studies are required to further investigate miR-1 as a novel target for the prevention and treatment of osteoarthritis.

Acknowledgments

Not applicable.

Funding

The present study was funded by the National Science Foundation for Young Scientists of China (grant no. 81601949), a Key Research and Development Project of Shanxi Province (grant no. 201803D421066), a Returned Overseas Students Research Funding Project of Shanxi Province (grant no. 2016-118), an Applied Basic Research Project of Shanxi Province (grant no. 201601D102067), and a Soft Science Research General Project of Shanxi Province (grant no. 2017041083-3).

Availability of data and materials

The datasets used and/or analyzed during the current study are available from the corresponding author on reasonable request.

Authors' contributions

PengcuiL, LW and XC conceived and designed the research. XC and XG drafted the manuscript. XC, XG, TC, YG, SL and PenghuaL performed the experiments. XC, XG, DS, CW and BL analyzed the data. XC, DS, and PengcuiL edited the article. All authors read and approved the final manuscript. All authors agree to be held accountable for all aspects of the study.

Ethics approval and consent to participate

The research protocol was approved by the Clinical Research Ethics Committee of Shanxi Medical University (approval no. 2019YX260), and the animal model experimental program

was approved by the Animal Experimental Ethics Committee of Shanxi Medical University (approval no. SYDL2019010). Each participant was required to obtain written informed consent before sample collection.

Patient consent for publication

Not applicable.

Competing interests

The authors declare that they have no competing interests.

References

- Glyn-Jones S, Palmer AJ, Agricola R, Price AJ, Vincent TL, Weinans H and Carr AJ: Osteoarthritis. *Lancet* 386: 376-387, 2015.
- Miller ME, Rejeski WJ, Messier SP and Loeser RF: Modifiers of change in physical functioning in older adults with knee pain: The observational arthritis study in seniors (OASIS). *Arthritis Rheum* 45: 331-339, 2001.
- Arden N and Nevitt MC: Osteoarthritis: Epidemiology. *Best Pract Res Clin Rheumatol* 20: 3-25, 2006.
- Berenbaum F: Osteoarthritis as an inflammatory disease (osteoarthritis is not osteoarthrosis!). *Osteoarthritis Cartilage* 21: 16-21, 2013.
- Araldi E and Schipani E: MicroRNA-140 and the silencing of osteoarthritis. *Genes Dev* 24: 1075-1080, 2010.
- Miyaki S, Sato T, Inoue A, Otsuki S, Ito Y, Yokoyama S, Kato Y, Takemoto F, Nakasa T, Yamashita S, *et al*: MicroRNA-140 plays dual roles in both cartilage development and homeostasis. *Genes Dev* 24: 1173-1185, 2010.
- Zhang X, Wang C, Zhao J, Xu J, Geng Y, Dai L, Huang Y, Fu SC, Dai K and Zhang X: MiR-146a facilitates osteoarthritis by regulating cartilage homeostasis via targeting Camk2d and Ppp3r2. *Cell Death Dis* 8: e2734, 2017.
- Guan YJ, Li J, Yang X, Du S, Ding J, Gao Y, Zhang Y, Yang K and Chen Q: Evidence that miR-146a attenuates aging- and trauma-induced osteoarthritis by inhibiting Notch1, IL-6, and IL-1 mediated catabolism. *Aging Cell* 17: e12752, 2018.
- Li YP, Wei XC, Li PC, Chen CW, Wang XH, Jiao Q, Wang DM, Wei FY, Zhang JZ and Wei L: The role of miRNAs in cartilage homeostasis. *Curr Genomics* 16: 393-404, 2015.
- Bagga S, Bracht J, Hunter S, Massirer K, Holtz J, Eachus R and Pasquinelli AE: Regulation by let-7 and lin-4 miRNAs results in target mRNA degradation. *Cell* 122: 553-563, 2005.
- Eulalio A, Rehwinkel J, Stricker M, Huntzinger E, Yang SF, Doerks T, Dorner S, Bork P, Boutros M and Izaurralde E: Target-specific requirements for enhancers of decapping in miRNA-mediated gene silencing. *Genes Dev* 21: 2558-2570, 2007.
- Valencia-Sanchez MA, Liu J, Hannon GJ and Parker R: Control of translation and mRNA degradation by miRNAs and siRNAs. *Genes Dev* 20: 515-524, 2006.
- Yuan X, Guo Y, Chen D, Luo Y, Chen D, Miao J and Chen Y: Long non-coding RNA MALAT1 functions as miR-1 sponge to regulate Connexin 43-mediated ossification of the posterior longitudinal ligament. *Bone* 127: 305-314, 2019.
- Li P, Wei X, Guan Y, Chen Q, Zhao T, Sun C and Wei L: MicroRNA-1 regulates chondrocyte phenotype by repressing histone deacetylase 4 during growth plate development. *FASEB J* 28: 3930-3941, 2014.
- Zhou J, Wei X and Wei L: Indian Hedgehog, a critical modulator in osteoarthritis, could be a potential therapeutic target for attenuating cartilage degeneration disease. *Connect Tissue Res* 55: 257-261, 2014.
- Lin AC, Seeto BL, Bartoszko JM, Khoury MA, Whetstone H, Ho L, Hsu C, Ali SA and Alman BA: Modulating hedgehog signaling can attenuate the severity of osteoarthritis. *Nat Med* 15: 1421-1425, 2009.
- Kirsch T, Swoboda B and Nah H: Activation of annexin II and V expression, terminal differentiation, mineralization and apoptosis in human osteoarthritic cartilage. *Osteoarthritis Cartilage* 8: 294-302, 2000.

18. Pfander D, Swoboda B and Kirsch T: Expression of early and late differentiation markers (proliferating cell nuclear antigen, syndecan-3, annexin VI, and alkaline phosphatase) by human osteoarthritic chondrocytes. *Am J Pathol* 159: 1777-1783, 2001.
19. Zhang C, Wei X, Chen C, Cao K, Li Y, Jiao Q, Ding J, Zhou J, Fleming BC, Chen Q, *et al*: Indian hedgehog in synovial fluid is a novel marker for early cartilage lesions in human knee joint. *Int J Mol Sci* 15: 7250-7265, 2014.
20. Orfanidou T, Iliopoulos D, Malizos KN and Tsezou A: Involvement of SOX-9 and FGF-23 in RUNX-2 regulation in osteoarthritic chondrocytes. *J Cell Mol Med* 13: 3186-3194, 2009.
21. Wei F, Zhou J, Wei X, Zhang J, Fleming BC, Terek R, Pei M, Chen Q, Liu T and Wei L: Activation of Indian hedgehog promotes chondrocyte hypertrophy and upregulation of MMP-13 in human osteoarthritic cartilage. *Osteoarthritis Cartilage* 20: 755-763, 2012.
22. Zhou J, Chen Q, Lanske B, Fleming BC, Terek R, Wei X, Zhang G, Wang S, Li K and Wei L: Disrupting the Indian hedgehog signaling pathway in vivo attenuates surgically induced osteoarthritis progression in Col2a1-CreERT2; Ihhf1/fl mice. *Arthritis Res Ther* 16: R11, 2014.
23. Guo L, Wei X, Zhang Z, Wang X, Wang C, Li P, Wang C and Wei L: Ipriflavone attenuates the degeneration of cartilage by blocking the Indian hedgehog pathway. *Arthritis Res Ther* 21: 109, 2019.
24. Lorenz J and Grassel S: Experimental osteoarthritis models in mice. *Methods Mol Biol* 1194: 401-419, 2014.
25. Jeon OH, Kim C, Laberge RM, Demaria M, Rathod S, Vasserot AP, Chung JW, Kim DH, Poon Y, David N, *et al*: Local clearance of senescent cells attenuates the development of post-traumatic osteoarthritis and creates a pro-regenerative environment. *Nat Med* 23: 775-781, 2017.
26. Altman R, Asch E, Bloch D, Bole G, Borenstein D, Brandt K, Christy W, Cooke TD, Greenwald R, Hochberg M, *et al*: Development of criteria for the classification and reporting of osteoarthritis. Classification of osteoarthritis of the knee. Diagnostic and therapeutic criteria committee of the American rheumatism association. *Arthritis Rheum* 29: 1039-1049, 1986.
27. Livak KJ and Schmittgen TD: Analysis of relative gene expression data using real-time quantitative PCR and the 2(-Delta Delta C(T)) method. *Methods* 25: 402-408, 2001.
28. Glasson SS, Chambers MG, Van Den Berg WB and Little CB: The OARSI histopathology initiative-recommendations for histological assessments of osteoarthritis in the mouse. *Osteoarthritis Cartilage* 18 (Suppl 3): S17-S23, 2010.
29. Ntziachristos V, Bremer C and Weissleder R: Fluorescence imaging with near-infrared light: New technological advances that enable in vivo molecular imaging. *Eur Radiol* 13: 195-208, 2003.
30. Peterson JD, Labranche TP, Vasquez KO, Kossodo S, Melton M, Rader R, Listello JT, Abrams MA and Misko TP: Optical tomographic imaging discriminates between disease-modifying anti-rheumatic drug (DMARD) and non-DMARD efficacy in collagen antibody-induced arthritis. *Arthritis Res Ther* 12: R105, 2010.
31. Selbach M, Schwanhauser B, Thierfelder N, Fang Z, Khanin R and Rajewsky N: Widespread changes in protein synthesis induced by microRNAs. *Nature* 455: 58-63, 2008.
32. Chen JF, Mandel EM, Thomson JM, Wu Q, Callis TE, Hammond SM, Conlon FL and Wang DZ: The role of microRNA-1 and microRNA-133 in skeletal muscle proliferation and differentiation. *Nat Genet* 38: 228-233, 2006.
33. Young B, Minugh-Purvis N, Shimo T, St-Jacques B, Iwamoto M, Enomoto-Iwamoto M, Koyama E and Pacifici M: Indian and sonic hedgehogs regulate synchondrosis growth plate and cranial base development and function. *Dev Biol* 299: 272-282, 2006.
34. Aigner T, Reichenberger E, Bertling W, Kirsch T, Stoss H and von der Mark K: Type X collagen expression in osteoarthritic and rheumatoid articular cartilage. *Virchows Arch B Cell Pathol Incl Mol Pathol* 63: 205-211, 1993.
35. Clements DN, Carter SD, Innes JF, Ollier WE and Day PJ: Analysis of normal and osteoarthritic canine cartilage mRNA expression by quantitative polymerase chain reaction. *Arthritis Res Ther* 8: R158, 2006.
36. Little CB, Barai A, Burkhardt D, Smith SM, Fosang AJ, Werb Z, Shah M and Thompson EW: Matrix metalloproteinase 13-deficient mice are resistant to osteoarthritic cartilage erosion but not chondrocyte hypertrophy or osteophyte development. *Arthritis Rheum* 60: 3723-3733, 2009.
37. Aigner T, Dietz U, Stoss H and von der Mark K: Differential expression of collagen types I, II, III, and X in human osteophytes. *Lab Invest* 73: 236-243, 1995.
38. Tchetina EV, Squires G and Poole AR: Increased type II collagen degradation and very early focal cartilage degeneration is associated with upregulation of chondrocyte differentiation related genes in early human articular cartilage lesions. *J Rheumatol* 32: 876-886, 2005.



This work is licensed under a Creative Commons Attribution-NonCommercial-NoDerivatives 4.0 International (CC BY-NC-ND 4.0) License.